of the interaction between bridging carbonyl ligands and aluminum alkyls has shown[30] that an adduct may form with the bridging carbonyl and AlR_3. An attempt to induce CO bridging in $Mn_2(CO)_{10}$ showed that such an adduct is not formed.[30] Consequently, the dibridged isomer of $Mn_2(CO)_{10}$ does not lie at low energy.

(30) Alich, A.; Nelson, N. J.; Strope, D.; Shriver, D. F. *Inorg. Chem.* **1972**, *12*, 2976-2983.

Acknowledgment. This material is based on work supported by the National Science Foundation under Grants No. CHE82-10514 (F.B.) and No. CHE84-02168 (W.C.T.). W.C.T. thanks the Alfred P. Sloan Foundation for a research fellowship. Helpful discussions with Prof. Charles Perrin, Prof. Roald Hoffmann, and Dr. Kevin Stewart are gratefully acknowledged.

A Mössbauer Effect Study of the Electronic Structure of Several Tetranuclear Organoiron Clusters

Christopher G. Benson, Gary J. Long,* John S. Bradley, J. W. Kolis, and D. F. Shriver

Contribution from the Departments of Chemistry, University of Missouri—Rolla, Rolla, Missouri 65401, Northwestern University, Evanston, Illinois 60201, and the Exxon Research and Engineering Company, Annandale, New Jersey 08801. *Received May 20, 1985*

Abstract: The Mössbauer spectra obtained at 78 K for a series of tetranuclear organoiron clusters reveal well-resolved quadrupole doublets with a range of average isomer shifts which may be related to the charge on the cluster. Single-crystal X-ray structural results are available for each of the clusters studied, and the Mössbauer spectra reveal the expected number of crystallographically distinct iron sites. The spectrum obtained for $(PPN)_2[Fe_4(CO)_{13}]$ (I), which contains a tetrahedral iron cluster with a triply-bridged carbonyl on one face, reveals a high electronic symmetry for the unique iron site. The remaining clusters have the butterfly structure and Mössbauer spectra which have clearly resolved doublets for the wingtip and backbone iron sites. The isomer shift values observed for each of the iron sites in several of the butterfly clusters is linearly related to the Slater effective nuclear charge experienced by the iron 4s electrons. The effective nuclear charge has been calculated from the orbital occupation values obtained through Fenske-Hall molecular orbital calculations published by Harris and Bradley. The results indicate that the Mössbauer effect isomer shift, when used in conjunction with detailed molecular orbital calculations, provides an accurate map of the electronic charge density distribution in a cluster. Further it provides insight into how this charge distribution changes with changes in the peripheral ligands in such a cluster.

The role played by surface bound carbon atoms in various metal catalyzed reactions has led to considerable interest in metal cluster chemistry.[1] The spectra of structurally characterized molecular metal clusters provide valuable reference points for the identification of surface species generated in the process of chemisorption and catalysis. Mössbauer effect spectra of organoiron clusters also may aid structural elucidation and provide insight into the electronic environment of the individual iron sites.

The Mössbauer effect spectra of the dianionic bipyramidal iron carbonyl cluster, $(PPN)_2[Fe_4(CO)_{13}]$ (I), and a series of neutral, monoanionic, and dianionic iron carbonyl butterfly clusters, II-VIII, have been measured and do indeed provide important clues to the electronic and structural nature of the clusters. Two previous Mössbauer effect studies of tetrameric iron carbonyl clusters have been reported.[2,3] Some of the present spectra duplicate those which were published earlier, but significantly different results were obtained for others.

Single-crystal X-ray structures are known for all of the compounds in the present study. In all cases, the Mössbauer data are both consistent with and complementary to the single-crystal X-ray structural results.

Experimental Section

All the clusters studied were prepared by using standard literature methods previously reported.[4-9] In all cases the samples were prepared, stored, handled, and measured under a nitrogen atmosphere or under vacuum at 78 K. Mössbauer effect spectra were obtained at 78 K on a conventional Ranger Scientific constant acceleration spectrometer which utilized a room temperature rhodium matrix cobalt-57 source and was calibrated at room temperature with natural abundance α-iron foil. The spectra were fit to Lorentzian line shapes by using standard least-squares computer minimization techniques. The error analysis was carried out by using standard error propagation techniques. In the spectral evaluation, the initial areas used for each iron component in an individual spectrum were based on the number of structurally distinct iron sites obtained from the single-crystal X-ray structure of the relevant cluster. With the exception of $(PPN)_2[Fe_4(CO)_{13}]$ (I), in which the areas of the two components were constrained in the fixed ratio of 3:1, all the components of each spectrum were allowed to vary, either as symmetric or asymmetric doublets, until the best fit was obtained.

Results and Discussion

The Mössbauer effect spectra were fit to quadrupole split doublets of independent areas and are shown in Figures 1 and 2. The resulting Mössbauer spectral parameters are listed in Table I. The value of $\sum\delta$ included in this table is the sum of the isomer shifts for each iron site in the cluster. The spectral fits are good, as indicated by the low χ^2 values and the goodness of fit illustrated in the figures. Under these conditions, the value of $\sum\delta$ is independent of spectral assignment. The value of $\Delta\delta$ is the shift in the isomer shift for a particular iron site in the cluster relative

(1) Muetterties, E. L.; Rhodin, T. N.; Band, E.; Brucker, C. F.; Pretzer, W. R. *Chem. Rev.* **1979**, *79*, 91-137.
(2) Farmery, K.; Kilner, M.; Greatrex, R.; Greenwood, N. N. *J. Chem. Soc. (A)* **1969**, 2339-2345.
(3) Sosinsky, B. A.; Norem, N.; Shelly, J. *Inorg. Chem.* **1982**, *21*, 348-356.
(4) Edgell, W. F.; Yang, M. T.; Bulkin, B. J.; Bayer, R.; Koizumi, N. *J. Am. Chem. Soc.* **1965**, *87*, 3080-3088.
(5) Tachikawa, M.,; Muetterties, E. L. *J. Am. Soc.* **1980**, *102*, 4541-4542.
(6) Holt, E. M.; Whitmire, K. H.; Shriver, D. F. *J. Organomet. Chem.* **1981**, *213*, 125-137.
(7) Manassero, M.; Sansoni, M.; Longoni, G. *J. Chem. Soc., Chem. Commun.* **1976**, 919-920.
(8) Bradley, J. S.; Ansell, G. B.; Hill, E. W. *J. Am. Chem. Soc.* **1979**, *101*, 7417-7419.
(9) Bradley, J. S.; Ansell, G. B.; Leonowicz, M. E.; Hill, E. W. *J. Am. Chem. Soc.* **1981**, *103*, 4968-4970.

0002-7863/86/1508-1898$01.50/0

Table I. Mössbauer Effect Spectral Parameters[a]

compound	site	δ	ΔE_Q	Γ_1	Γ_2	% area	χ^2	$\Delta\delta$	$\sum\delta$
$(PPN)_2[Fe_4(CO)_{13}]$ (I)	Fe(4)	0.044 (4)	0[b]	0.273 (4)		25.0[b]	1.07		0.06 (1)
	Fe(1,2,3)	0.006 (4)	0.397 (2)	0.263 (3)	0.263 (3)	75.0[b]			
$(BzNMe_3)_2[Fe_4(CO)_{12}C]$ (II)	Fe(1,4)	−0.107 (4)	1.118 (6)	0.284 (3)	0.300 (3)	51.6	0.96	0	−0.24 (1)
	Fe(2,3)	−0.015 (4)	0.462 (3)	0.278 (2)	0.288 (3)	48.4		0	
$(PPN)[HFe_4(CO)_{12}C]$ (III)	Fe(1,4)	−0.019 (4)	0.806 (4)	0.301 (4)	0.301 (4)	54.3	1.46	0.088 (6)	−0.22 (1)
	Fe(2,3)	−0.091 (4)	1.433 (7)	0.281 (3)	0.281 (3)	45.7		−0.076 (6)	
$(PPN)[HFe_4(CO)_{12}(\eta^2\text{-CO})]$ (IV)	Fe(1)	0.030 (4)	1.940 (9)	0.240 (4)	0.240 (4)	25.9	0.85	0.137 (6)	0.29 (1)
	Fe(4)	0.076 (4)	0.736 (3)	0.240 (3)	0.222 (3)	24.8		0.183 (6)	
	Fe(2,3)	0.093 (4)	0.684 (4)	0.283 (3)	0.283 (3)	49.3		0.108 (6)	
$(Et_4N)[Fe_4(CO)_{12}CCOMe]$ (V)	Fe(1,4)	−0.017 (4)	0.267 (2)	0.234 (2)	0.270 (2)	45.8	1.03	0.090 (6)	−0.08 (1)
	Fe(2,3)	−0.023 (4)	0.614 (3)	0.262 (2)	0.274 (2)	54.2		−0.008 (6)	
$(Et_4N)[Fe_4(CO)_{12}CCO_2Me]$ (VI)	Fe(1,4)	−0.017 (4)	0.256 (1)	0.331 (2)	0.314 (2)	58.0	1.32	0.090 (6)	−0.07 (1)
	Fe(2,3)	−0.017 (4)	0.640 (3)	0.244 (2)	0.254 (2)	42.0		−0.002 (6)	
$HFe_4(CO)_{12}(\eta^2\text{-CH})$ (VII)	Fe(1)	−0.034 (5)	1.553 (9)	0.267 (2)	0.267 (2)	28.8	1.08	0.073 (6)	−0.03 (1)
	Fe(4)	−0.001 (5)	0.572 (4)	0.223 (2)	0.223 (2)	26.4		0.106 (6)	
	Fe(2,3)	0.002 (5)	0.772 (4)	0.269 (2)	0.269 (2)	44.8		0.017 (6)	
$Fe_4(CO)_{13}C$ (VIII)	Fe(1,4)	−0.044 (4)	1.890 (10)	0.266 (3)	0.262 (3)	48.0	1.23	0.060 (6)	−0.01 (1)
	Fe(2,3)	0.041 (4)	1.604 (8)	0.282 (3)	0.290 (3)	52.0		0.056 (6)	

[a] All data in mm/s obtained at 78 K relative to room temperature natural abundance α-iron foil. [b] Component variable constrained to the given value.

Chart I

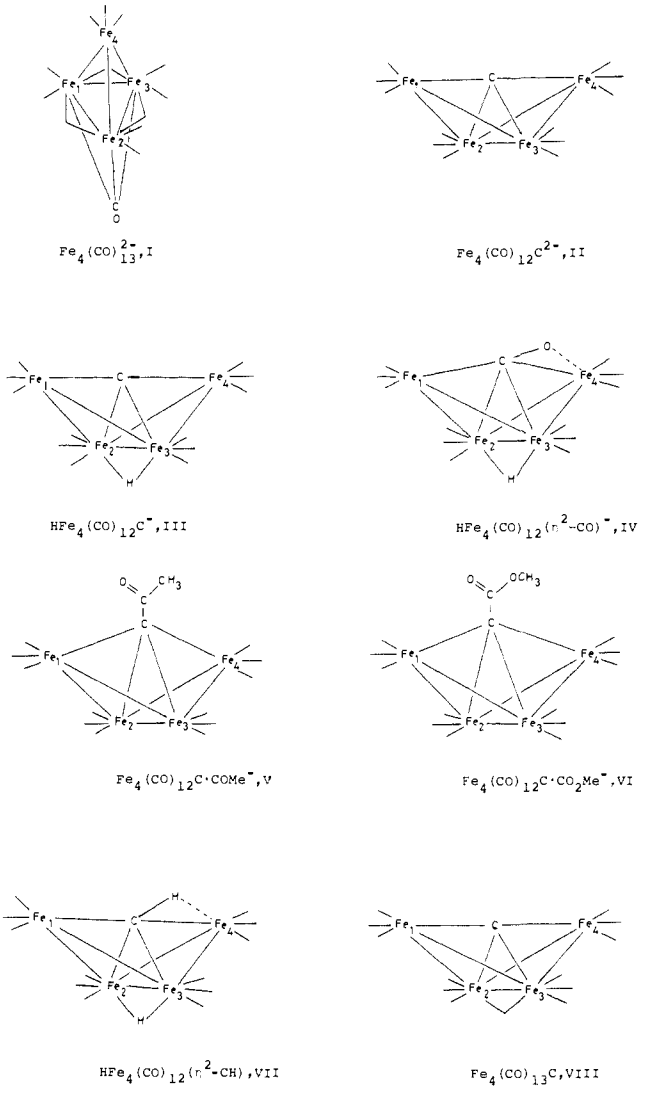

to the reference cluster (see below), $[Fe_4(CO)_{12}C]^{2-}$ (II). The values of $\Delta\delta$ are, of course, very dependent upon the validity of our assignment of a spectral component to a specific iron site in the cluster.

The Mössbauer spectrum of $[Fe_4(CO)_{13}]^{2-}$ (**I**) was previously reported by Farmery et al.[2] While our results are consistent with theirs, our purpose in reporting them here is twofold. First, our

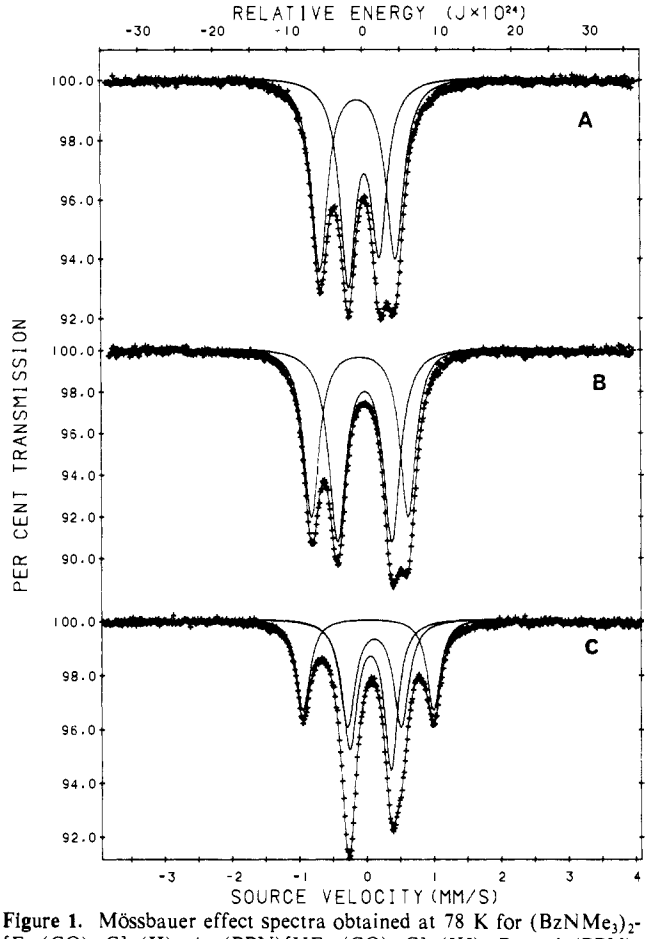

Figure 1. Mössbauer effect spectra obtained at 78 K for $(BzNMe_3)_2[Fe_4(CO)_{12}C]$ (II), A; $(PPN)[HFe_4(CO)_{12}C]$ (III), B; and $(PPN)[HFe_4(CO)_{12}(\eta^2\text{-CO})]$ (IV), C.

fitting technique allows us to distinguish between the two distinct iron sites, and second, this bipyramidal cluster provides a useful comparison to the structurally very different butterfly clusters discussed herein.

The X-ray structure of $[Fe_4(CO)_{13}]^{2-}$ (I), reported by Doedens and Dahl,[10] shows a bipyramidal structural with three equivalent basal iron sites, Fe(1,2,3), and one triply bridged apical iron site, Fe(4). The second apex consists of a triply bridged carbonyl ligand as illustrated in I. The Mössbauer spectrum of I reveals an essentially symmetric electronic environment for the unique apical

(10) Doedens, R. J.; Dahl, L. F. *J. Am. Chem. Soc.* **1966**, *88*, 4847–4855.

Table II. Calculated Electronic Configurations for the Organoiron Clusters

cluster	site	iron orbital occupation 3d	4s	4p	overlap populations[a] $C2p_x$	$C2p_y$	$C2p_z$	iron charge	carbon[b] charge	hydrogen charge	Z_{eff}[c]
$[Fe_4(CO)_{12}C]^{2-}$ (II)	Fe(1,4)	6.53	0.41	0.97		0.038		0.10	−0.60		3.310
	Fe(2,3)	6.57	0.44	0.92	0.018		0.028	0.07			3.294
$[HFe_4(CO)_{12}C]^-$ (III)	Fe(1,4)	6.59	0.41	0.91		0.039		0.10	−0.65	−0.26	3.280
	Fe(2,3)	6.61	0.39	0.79	0.015		0.021	0.20			3.305
$[Fe_4(CO)_{12}CCO_2Me]^-$ (VI)	Fe(1,4)	6.66	0.40	0.77		0.017	0.005	0.17	−0.69		3.270
	Fe(2,3)	6.61	0.44	0.90	0.026		0.019	0.04			3.267
$Fe_4(CO)_{13}C$ (VIII)	Fe(1,4)	6.62	0.40	0.83		0.037		0.15	−0.66		3.282
	Fe(2,3)	6.67	0.38	0.85	0.015		0.023	0.10			3.233

[a] The overlap population of the iron 4s function with the appropriate carbide or bridging carbon 2p function. [b] The charge on the carbide or bridging carbon atom. [c] The effective nuclear charge (see text) experienced by the iron 4s electrons.

Fe(4) as indicated by the lack of a quadrupole interaction for this site. Apparently the three Fe(4) to Fe(1,2,3) bonds resemble electronically the three Fe(4) to terminal carbonyl bonds. A very similar result is found for the unique iron site in $Fe_3(CO)_{12}$.[11] The basal iron sites show the expected small electronic asymmetry. The isomer shifts for each of these sites and hence $\sum\delta$ is quite large for this type of dicationic cluster.[11] In general, the higher the iron-57 Mössbauer effect isomer shift the lower is the s-electron density at the iron nucleus. The relatively high value suggests to us that the negative charge of the cluster is primarily associated with the apical triply bridged carbonyl moiety. This is not an unreasonable assumption. Harris and Bradley,[12] in a recent Fenske–Hall molecular orbital study of several iron butterfly clusters, have shown that there is an approximate negative charge of −0.6 associated with the carbide carbon in $[Fe_4(CO)_{12}C]^{2-}$ (II). Their study[12] and its relation to the Mössbauer spectra of the butterfly clusters will be dealt with in more detail below.

The Mössbauer spectra of $[HFe_4(CO)_{12}(\eta^2\text{-}CO)]^-$, $[Fe_4(CO)_{12}C]^{2-}$, $[HFe_4(CO)_{12}C]^-$, and $HFe_4(CO)_{12}(\eta^2\text{-}CH)$ have been reported.[2,3] The compound, $[HFe_4(CO)_{12}(\eta^2\text{-}CO)]^-$ (IV) was studied by Farmery et al.[2] before the determination of its X-ray structure. At that time its structure was thought to contain a face-bridging CO similar to that observed in $[Fe_4(CO)_{13}]^{2-}$ (I). The structure was, however, later shown[7] to be of the butterfly type, IV. In general, our results are consistent with those of Farmery et al.,[2] although they report a considerable degree of variation in the outer quadrupole doublet which we do not observe. The results which we obtained for $[Fe_4(CO)_{12}C]^{2-}$ (II), $[HFe_4(CO)_{12}C]^-$ (III), and $HFe_4(CO)_{12}(\eta^2\text{-}CH)$ (VII) are very different from those reported in a study of Sosinsky et al.[3] We suspect that the differences may be related to the very air sensitive nature of the clusters. In all of our studies, the materials were carefully protected from exposure to oxygen or vacuum at room temperature. Such exposure leads to broad unresolved spectra similar to those reported earlier.[3]

We recently reported[11] a Mössbauer effect study of $Fe_3(CO)_{12}$, $(PPN)[Fe_3(CO)_{10}(CH)]$, $(PPN)[Fe_2Co(CO)_9(CCO)]$, and $(PPN)_2[Fe_3(CO)_9(CCO)]$. Our approach was to use the neutral $Fe_3(CO)_{12}$ cluster as a reference cluster such that comparisons could be made with the isomer shifts of the other clusters. While there is no known neutral tetranuclear iron cluster which could be used as such a reference, it is possible to use $[Fe_4(CO)_{12}C]^{2-}$ (II) in a similar manner.

The spectral parameters for all the tetrairon "butterfly" clusters are given in Table I. As indicated above, $\Delta\delta$ is the change in isomer shift from the reference $[Fe_4(CO)_{12}C]^{2-}$ and $\sum\delta$ is the sum of the relative isomer shifts for each iron site. The analysis of a given spectrum has two aspects which must be considered together. First the individual lines in the spectrum must be assigned to a specific quadrupole doublet. In some cases, the intensity of the individual lines makes the assignment quite obvious, as is the case in Figures 1C and 2C. In other cases this doublet assignment is less obvious, at least for initial trial fits. To cope with this problem, the range of possible isomer shift values is minimized. This of course corresponds to "nested" quadrupole doublets. In the current case this minimization of isomer shift values is justified by the results of theoretical calculations[12] which indicate very similar 4s and 3d orbital populations for these clusters. The second aspect involves the assignment of a specific quadrupole doublet in the observed spectrum to a specific iron site in the cluster. This assignment, which has proven quite difficult in the current work, involved both the evaluation of the individual iron site symmetry

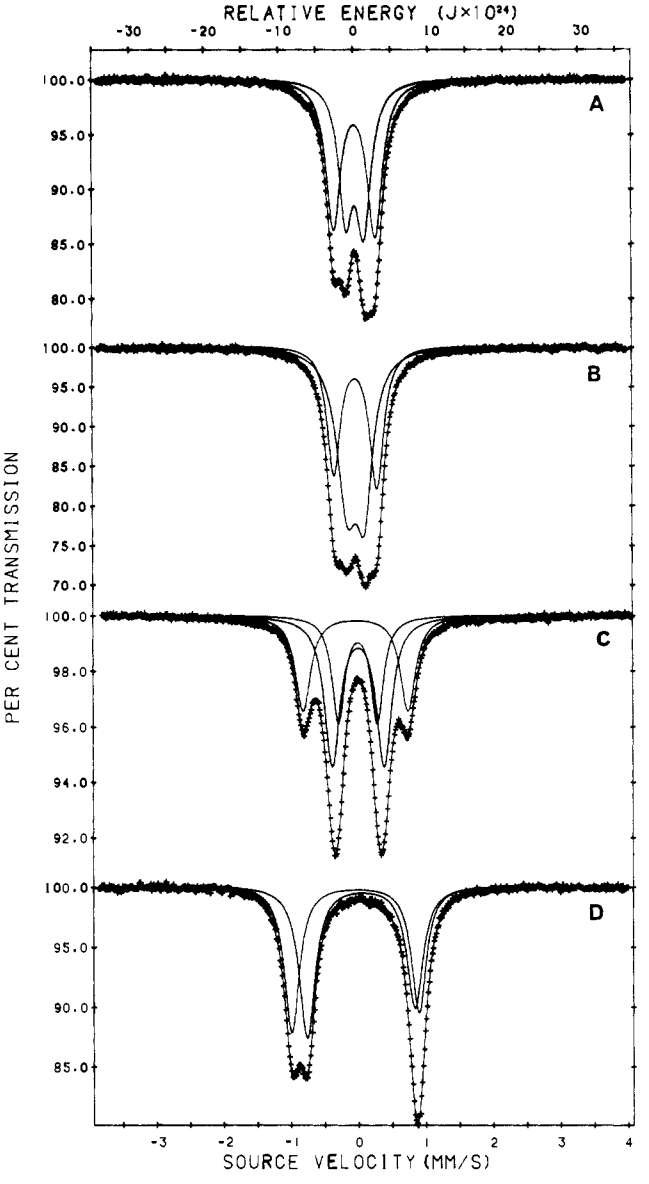

Figure 2. Mössbauer effect spectra obtained at 78 K for $(Et_4N)[Fe_4(CO)_{12}CCOMe]$ (V), A; $(Et_4N)[Fe_4(CO)_{12}CCO_2Me]$ (VI), B; $HFe_4(CO)_{12}(\eta^2\text{-}CH)$ (VII), C; and $Fe(CO)_{13}C$ (VIII), D.

(11) Benson, C. G.; Long, G. J.; Kolis, J. W.; Shriver, D. F. *J. Am. Chem. Soc.* **1985**, *107*, 5297–5298.
(12) Harris, S.; Bradley, J. S. *Organometallics* **1984**, *3*, 1086–1093.

Table III. Iron-Carbon Bond Lengths for the Butterfly Clusters[a]

cluster	Fe_w-C[b] Fe(1)	Fe_w-C[b] Fe(4)	Fe_b-C[c] Fe(2)	Fe_b-C[c] Fe(3)	Fe_w-C-Fe_w,[d] deg	Fe(2)-Fe(3) bond length	dihedral angle, deg	ref
$[Fe_4(CO)_{12}C]^{2-}$ (II)	1.772	1.803	1.936	1.969	178	2.521	101	15
$[HFe_4(CO)_{12}C]^-$ (III)	1.790	1.790	1.990	1.990	174	2.608	104	6
$[HFe_4(CO)_{12}(\eta^2\text{-}CO)]^-$ (IV)	1.810	2.170	2.100	2.100		2.627	117	7
$[Fe_4(CO)_{12}CCOMe]^-$ (V)	2.011	2.008	1.964	1.970	147	2.572	128	19
$[Fe_4(CO)_{12}CCO_2Me]^-$ (VI)	2.027	2.012	1.957	1.952	148	2.590	130	8
$HFe_4(CO)_{12}(\eta^2\text{-}CH)$ (VII)	1.927	1.827	1.949	1.941	171	2.604	111	17
$Fe_4(CO)_{13}C$ (VIII)	1.797	1.800	1.998	1.987	175	2.545	101	9

[a] Bond lengths in Å. [b] Wingtip iron to carbide or bridging carbon bond length. [c] Backbone iron to carbide or bridging carbon bond length. [d] Wingtip iron(1)-carbide or bridging carbon-wingtip iron(4) bond angle.

and the electronic environment at the site. The Fenske-Hall molecular orbital calculations of Harris and Bradley[12] were most helpful in making these assignments. Selected results of these calculations are presented in Table II.

We will begin our discussion of the results by noting that the values of $\sum\delta$ which are independent of site assignment (see Experimental Section), fall into distinct groups depending on the charge of the cluster. The similar $\sum\delta$ values of −0.24 and −0.22 mm/s found for the dianion $[Fe_4(CO)_{12}C]^{2-}$ (II) and the monoanion $[HFe_4(CO)_{12}C]^-$ (III), respectively, indicate very similar electronic environments for these two clusters as has been noted earlier.[12] In fact, the similar $\sum\delta$ values indicate that III might better be considered as the dianion cluster $(H)^+[Fe_4(CO)_{12}C]^{2-}$. The monoanionic clusters $[Fe_4(CO)_{12}CCOMe]^-$ (V) and $[Fe_4(CO)_{12}CCO_2Me]^-$ (VI) have the expected similar values of −0.08 and −0.07 mm/s, respectively, for $\sum\delta$. The neutral clusters $HFe_4(CO)_{12}(\eta^2\text{-}CH)$ (VII) and $Fe_4(CO)_{13}C$ (VIII) have the larger values of $\sum\delta$ of −0.03 and −0.01 mm/s, respectively. This increase in isomer shift sum upon the reduction of the negative charge on the cluster is similar to that observed[11] for some related trinuclear organoiron clusters and corresponds to the reduction of the net s-electron density at the iron nucleus upon oxidation. Therefore, it is quite surprising to find that the monoanionic cluster $[HFe_4(CO)_{12}(\eta^2\text{-}CO)]^-$ (IV) has the highest observed $\sum\delta$ value of 0.29 mm/s.

As noted above and in Table II, each of the clusters for which extended calculations are available have very similar iron 4s orbital occupations. The small range of values of 0.38 to 0.44 and the inherent error in these values do not allow their use for the direct assignment of a spectral component to an iron site in a given cluster. Further, such a basis for assignments would not account for deshielding effects from π bonding. We have found that the best approach is to use the iron valence orbital occupancies to calculate an effective nuclear charge, Z_{eff}, by using the method of Slater.[13,14] The results of this calculation for the iron 4s electron are included in Table II and a plot of isomer shift vs. Z_{eff} is shown in Figure 3. The linear least-squares fit to the data gives a slope of −1.736 mm/s*charge, an isomer shift intercept of 5.660 mm/s, and a correlation coefficient of 0.91. The results show the expected and fairly consistent drop in iron-57 isomer shift with increasing effective nuclear charge. In all instances, the assignments presented in Table I have been used in Figure 3, and except for cluster VI, the alternative assignments do not show the expected correlation. It is gratifying that in $[Fe_4(CO)_{12}CCO_2Me]^-$ (VI) the two iron sites, which have the same isomer shift, also have virtually the same effective nuclear charge.

The quadrupole splittings for the different types of iron in $[Fe_4(CO)_{12}C]^{2-}$ (II) reveal the presence of a substantial electric field gradient at the "wingtip" iron as a result of the presence of the bonding to the carbide. The "backbone" iron sites have a smaller electronic asymmetry, perhaps because of the substantially longer Fe(2,3) to carbide bond length. Selected cluster bond distances and angles are presented in Table III.

Upon protonation of $[Fe_4(CO)_{12}C]^{2-}$ (II) to form $[HFe_4(CO)_{12}C]^-$ (III) there is little change in $\sum\delta$, whereas the "wingtip" Fe(1,4) isomer shift increases slightly with a $\Delta\delta$ of 0.088 mm/s and the "backbone" Fe(2,3) isomer shift decreases slightly with a $\Delta\delta$ value of −0.076 mm/s. These small changes are consistent with changes in Z_{eff} and the theoretical molecular orbital calculations.[12] These calculations show that there are only small changes in the electronic structure upon conversion of II to III. The structral changes within the cluster, with the exception of the Fe(2)-Fe(3) bond distances, are also small (see Table III). The major electronic changes are the loss of the $6a_1$ HOMO in II and the appearance at about 6 eV lower in energy of a new $1a_1$ orbital in III. The $6a_1$ orbital is bonding between Fe(2) and Fe(3) and is mainly localized between these "backbone" iron atoms. The new lower energy $1a_1$ orbital in III is the bonding combination of the $6a_1$ orbital of II with the hydrogen 1s orbital. The formation of the hydrogen bridge has resulted in a substantial decrease in the overlap populations of the two backbone iron atoms and a resultant increase of the Fe(2)-Fe(3) distance from 2.521 Å in II to 2.608 Å in III. The decrease in Fe(2)-Fe(3) orbital overlap population and the presence of the −0.26 charge on the bridging hydrogen results in the reduced occupany of the iron 4s orbital, a high s-electronic density at the nucleus, and the reduced isomer shift for the backbone Fe(2,3) site. The presence of the bridging hydrogen does introduce a substantial increase in the electric field gradient experienced by this site and the quadrupole interaction increases from 0.462 mm/s in II to 1.433 mm/s in III. It is harder to account for the increase in isomer shift for the "wingtip" iron sites, but it may be associated with changes in the Fe(1)-Fe(2) and Fe(3)-Fe(4) bonding which occurs through the $5b_2$ HOMO in III.

Upon oxidation of $[Fe_4(CO)_{12}C]^{2-}$ (II) in the presence of carbon monoxide, the neutral molecule $Fe_4(CO)_{13}C$ (VIII) is formed with the added carbonyl group bridging the backbone Fe(2) and Fe(3) atoms. Once again the electronic and structural properties of the cluster remain much the same as that found in II.[9,12] The only real difference is a further decrease in the energy of the $6a_1$ orbital of II as it interacts with the 5σ orbital of the bridging carbonyl

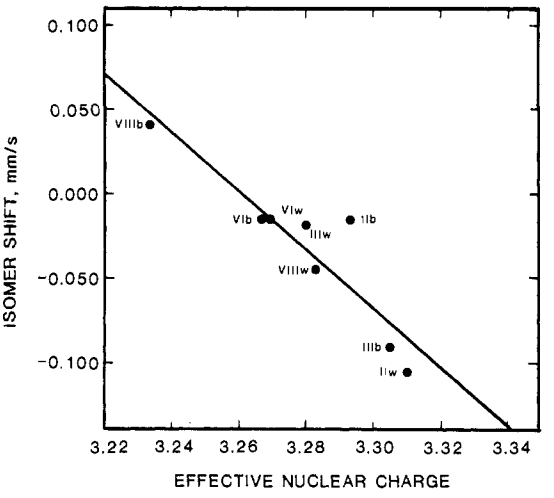

Figure 3. A plot of the Slater effective nuclear charge vs. the isomer shift for several butterfly clusters. The errors associated with the isomer shift are ca. twice the size of the points.

(13) Slater, J. C. *Phys. Rev.* **1930**, *36*, 57–64.
(14) Huheey, J. E. "Inorganic Chemistry", 3rd ed.; Harper and Row: New York; 1983, p 37.

group. However, in this case, in spite of a decrease in the overlap populations between the backbone iron atoms, there is only an ca. 0.024 Å increase in the Fe(2)–Fe(3) distance (as compared with a 0.087 Å increase in III, see Table III). The Mössbauer isomer shift values reflect these changes directly. The wingtip iron isomer shift change, $\Delta\delta$, is virtually the same as that observed in III. However, the change in the backbone iron isomer shift, $\Delta\delta$, upon oxidation and carbonylation of II to form VIII shows a small positive shift of 0.056 mm/s. Apparently the strong interaction of the $6a_1$ orbital originating in II with the carbonyl permits the expansion of the 4s functions yielding the increase in isomer shift. The influence of the bridging carbonyl is also seen in the large increase in the quadrupole interaction on the backbone site in VIII as compared with II and III.

As is illustrated in Figure 2, both $[Fe_4(CO)_{12}CCO_2Me]^-$ (VI) and $[Fe_4(CO)_{12}CCOMe]^-$ (V) exhibit quite different spectra than the butterfly clusters discussed so far. The reaction of $Fe_4(CO)_{13}C$ (VIII) with a nucleophile such as CH_3OH involves a structural change in the Fe_4C framework,

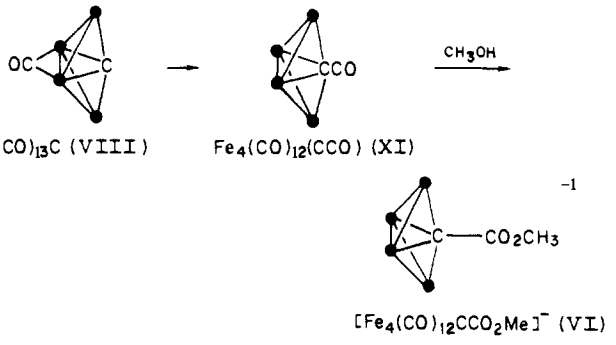

and is believed[15] to proceed via the ketenylidene intermediate, IX. The original carbido carbon atom is pulled away from the wingtip Fe(1)–Fe(4) vector, lengthening the Fe(1,4)–C bond lengths from ca. 1.79 Å in II, III, and VIII to ca. 2.01 Å in V and VI. This is accompanied by a decrease in the Fe(1)–C–Fe(4) bond angle from ca. 176° to 148° in VI and an opening of the butterfly dihedral angle from ca. 101° to 130° in VI. There is also a significant decrease in the average wingtip to backbone iron distance from 2.64 Å in II to 2.50 Å in VI. In contrast, there is almost no change in the carbon to backbone iron bond length, the average being 1.98 Å in II, III, and VIII and 1.96 Å in V and VI. These structural changes have been shown[12] to have a marked effect on the bonding between the bridging carbon 2p orbitals and the wingtip iron 3d, 4s, and 4p orbitals, the σ and π interactions being drastically reduced, whereas the σ interaction with the backbone iron atoms remains virtually unchanged. This is most easily seen in the iron 4s to carbon 2p orbital overlap populations given in Table II. The total σ overlap with Fe(2,3) is 0.046 in II and 0.045 in VI. In contrast, the value for Fe(1,4) decreases from 0.038 in II to 0.022 in VI. Similar changes would be expected in V. Hence it is not surprising that the isomer shift for the Fe(2,3) backbone site remains virtually unchanged upon conversion of II into V and VI, the $\Delta\delta$ being −0.008 and −0.002 mm/s, respectively. Similarly, the quadrupole interaction for this site increases by only ca. 0.2 mm/s relative to II. In contrast, the wingtip Fe(1,4) sites show an increase in isomer shift relative that of II, the value of $\Delta\delta$ being 0.090 mm/s in each case. This shift must result from the extensive loss of the π interaction[12] between the carbido carbon $2p_x$ and $2p_z$ orbital and the wingtip iron orbitals. The decreased radial function for the iron 3d and 4p functions would further shield the 4s electrons, decreasing the effective nuclear charge, decreasing the 4s density at the iron nucleus, and increasing the isomer shift relative to that found in II.

Another consequence of the movement of the carbido carbon atom and the change in the butterfly dihedral angle is to provide more "flexibility" to the bonding at the wingtip iron sites. Apparently this results in a decrease in the electric field gradient at the nucleus yielding a very small quadrupole interaction for these sites in both V and VI.

Although a detailed molecular orbital study has not been carried out on $[Fe_4(CO)_{12}CCOMe]^-$ (V), similar trends in $\Delta\delta$ and $\sum\delta$ are observed and there appears to be no reason why the same electronic arguments should not apply.

Another molecular orbital study of $HFe_4(CO)_{12}(\eta^2\text{-CH})$ (VII) has been carried out by Housecroft and Fehlner.[16] In that study the interaction of the η^2-CH ligand with the wingtip iron sites was studied by using the Fenske–Hall method. The results show that there is a small preference in bonding terms for the tilting of the C–H group toward one of the wingtip iron sites as has been shown to be the case in both X-ray[5] and neutron diffraction studies.[17] It was also found that, as a direct consequence of the tilting, there is an acceptance of electronic charge from the wingtip Fe(4), to which the methyne hydrogen is bound, into an empty 3σ antibonding orbital belonging to the methyne hydrogen. The Mössbauer spectral parameters for $HFe_4(CO)_{12}(\eta^2\text{-CH})$ (VII) illustrate this point very well. The isomer shift for the wingtip Fe(1) site not bound to the methyne hydrogen is similar to that for the wingtip Fe(1,4) sites in the neutral $Fe_4(CO)_{13}C$ cluster, VIII, discussed above. However, the Fe(4) wingtip site shows a larger isomer shift suggesting a loss in s-electron density consistent with that predicted in the molecular orbital study.[16] Once again, the isomer shift for the backbone Fe(2,3) sites is very similar to that found in II, the $\Delta\delta$ value being only 0.017 mm/s. Also, as expected, the bridging proton in VIII reduces the quadrupole interaction at the Fe(4) site while the other sites have values similar to those in II.

The results obtained for $[HFe_4(CO)_{12}(\eta^2\text{-CO})]^-$ (IV) are more difficult to explain than those of the other butterfly clusters studied herein. The isomer shift and $\Delta\delta$ values for each of the iron sites are all very large and positive as is $\sum\delta$. These high values may be explained by assuming that a greater proportion of the cluster negative charge is associated with the η^2-CO moiety than for the other clusters. This would account for the larger value of $\sum\delta$ and the very low carbonyl stretching frequency of ca. 1390 cm^{-1} found[18] for the η^2-CO ligand. The large isomer shift assigned to the wingtip Fe(4) site bound to both the carbon and oxygen atoms of the η^2-CO may be explained in a manner similar to that for the $HFe_4(CO)_{12}(\eta^2\text{-CH})$ (VII) cluster discussed above. Hence it seems likely that there is movement of s-electron density away from the wingtip Fe(4) toward the oxygen of the η^2-CO. Further evidence for this is found in the increase[7] in the Fe(4)–C bond length to 2.17 Å as compared with 1.81 Å for the Fe(1)–C bond length. In fact, all the iron–carbon bond lengths, with the exception of Fe(1)–C, are longer and presumably weaker in $[HFe_4(CO)_{12}(\eta^2\text{-CO})]^-$ (IV) than in any of the other clusters in this study (see Table III). The large quadrupole splittings found in $[HFe_4(CO)_{12}(\eta^2\text{-CO})]^-$ (IV) reflect the decreased symmetry at the iron sites resulting from the η^2-CO in the cluster. This result is similar to the asymmetry induced by η^2-CH in VII.

Conclusions

Mössbauer effect hyperfine parameters are a very sensitive way to study the electronic structures of complex organoiron clusters. However, due care is required to ensure that the materials are pure at the time of measurement. The resulting hyperfine parameters, and in particular the Mössbauer effect isomer shift, when used in conjunction with detailed molecular orbital calculations for such clusters, can provide an accurate map of the relative changes in electronic density within a variety of clusters as chemistry is carried out on the peripheral organic ligands. Perhaps most important, the hyperfine parameters complement molecular

(15) Bradley, J. S. *Phil. Trans. R. Soc., London* **1982**, *A308*, 103–113.

(16) Housecroft, C. E.;: Fehlner, T. P. *Organometallics* **1983**, *2*, 690–692.

(17) Beno, M. A.; Williams, J. M.; Tachikawa, M.; Muetterties, E. L. *J. Am. Chem. Soc.* **1981**, *103*, 1485–1492.

(18) Horwitz, C. P.; Holt, E. M.; Shriver, D. F. *J. Am. Chem. Soc.* **1985**, *107*, 281–282.

(19) Bradley, J. S.; Harris, S.; Hill, E. W.; Leta, S. *Organometallics*, submitted for publication.

orbital studies. Specifically, the total isomer shift values for a series of clusters provides a measure of the relative charge associated with the iron cluster framework. Finally, there is a direct relationship between the isomer shift and the Slater effective nuclear charge experienced by the iron 4s electrons.

Acknowledgment. The authors thank Dr. J. M. Williams of Argonne National Laboratory for a small sample of $HFe_4(CO)_{12}(\eta^2\text{-}CH)$ (VII), which was used in his neutron diffraction studies.[17] It gave results identical with those of the sample prepared at Northwestern University and used in this study. We thank the donors of the Petroleum Research Fund, administered by the American Chemical Society, for their support of this research. Sample preparation at Northwestern University was supported by the National Science Foundation. We thank Joseph Hriljac for some of the samples and Drs. S. Harris, C. E. Housecroft, T. P. Fehlner, H. Kaesz, and F. Grandjean for many helpful discussions during the course of this work.

Registry No. I, 69665-30-1; II, 80063-51-0; III, 74792-03-3; IV, 77674-97-6; V, 99922-06-2; VI, 72872-04-9; VII, 76547-44-9; VIII, 79061-73-7.

Copper–Catechol Chemistry. Synthesis, Spectroscopy, and Structure of Bis(3,5-di-*tert*-butyl-*o*-semiquinato)copper(II)

Jeffery S. Thompson* and Joseph C. Calabrese

Contribution No. 3865 from the Centeral Research and Development Department, E. I. du Pont de Nemours & Company, Experimental Station, Wilmington, Delaware 19898.
Received September 5, 1985

Abstract: The synthesis, spectroscopy, structure, and reactivity of bis(3,5-di-*tert*-butyl-*o*-semiquinato)copper(II), $Cu(DTBSQ)_2$, a Cu(II)–semiquinone complex, are presented. This compound was prepared by reacting $[Cu(pyridine)_4]X$ (X = ClO_4, Cl) with the corresponding benzoquinone or a basic Cu(II) dimer, $[Cu_2(pyridine)_4(OCH_3)_2](ClO_4)_2$, with the catechol. The complex, which was characterized by analytical, spectroscopic, and X-ray diffraction techniques, crystallizes in the triclinic space group $P\bar{1}$ with $Z = 2$ in a unit cell of dimensions $a = 10.262$ (3) Å, $b = 14.554$ (4) Å, $c = 9.418$ (2) Å, $\alpha = 101.09$ (2)°, $\beta = 92.31$ (2)°, $\gamma = 108.87$ (2)° at −100 °C. Least-squares refinement of 298 variables led to a value of the conventional R index of 0.049 and $R_w = 0.046$ for 2296 reflections having $I > 3\sigma(I)$. Each copper ion is coordinated to four oxygen atoms from two DTBSQ ligands. In addition, there is a fifth oxygen atom from a neighboring $Cu(DTBSQ)_2$ molecule coordinated to the copper atom in an axial position; thus, the overall geometry about the metal ion approaches square pyramidal. The C–O bond lengths of the DTBSQ ligands range from 1.290 (7) to 1.296 (6) Å. The spectroscopic properties and reactions of $Cu(DTBSQ)_2$ are consistent with the Cu(II)–semiquinone formulation. These results suggest that the copper oxidation of catechols takes place in two one-electron-transfer steps.

In this contribution, we present the synthesis, spectroscopy, structure, and reactivity of a Cu(II)–3,5-di-*tert*-butyl-*o*-semiquinone (DTBSQ) complex that gives considerable insight into how copper ions oxidize catechols to quinones. This reaction has been of considerable interest for many years because of its synthetic utility and relevance to biological systems.[1-3] The cupric ion clearly functions as an electron acceptor in this oxidation reaction. Dioxygen is used to reoxidize cuprous ion produced during the catalytic reaction but is not necessary for substrate oxidation.[1-3] To date, no copper–catechol species from catalytically active mixtures, which usually consist of cuprous chloride in a pyridine–methanol solvent mixture, have been isolated and characterized, yet several structures have been proposed for the copper-containing intermediates,[1-3] and a simultaneous, two-electron transfer from the catecholate ion to two cupric ions has been suggested as a critical step in the oxidation of catechol to benzoquinone.[1,2]

Our work reported here and elsewhere[4] suggests that this oxidation reaction proceeds in two one-electron-transfer steps with a semiquinone intermediate (eq 1), rather than a single two-electron-transfer step. We recently reported the syntheses and

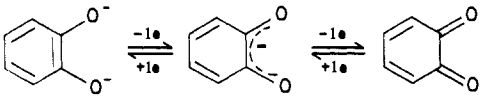

(1)

structures of a series of Cu(II)–DTBSQ complexes prepared by reacting di-μ-methoxy- or di-μ-hydroxydicopper(II) compounds with the catechol (eq 2) or by reacting Cu(I)–ethylene complexes with the corresponding benzoquinone, DTBBQ (eq 3).[4] Bidentate

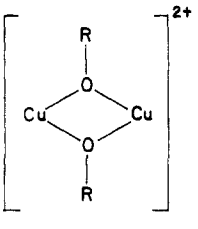

+ DTBC ⟶ [Cu(DTBSQ)]$^+$ + Cu(I) (2)

nitrogen-donating ligands are used as the other ligands in the

(1) Rogic, M. M.; Swerdloff, M. D.; Demmin, T. R. In "Copper Coordination Chemistry: Biochemical and Inorganic Perspectives"; Karlin, K. D., Zubieta, J., Eds.; Adenine Press: New York, 1983; pp 259–279.
(2) (a) Demmin, T. R.; Swerdloff, M. D.; Rogic, M. M. *J. Am. Chem. Soc.* **1981**, *103*, 5795–5804. (b) Rogic, M. M.; Demmin, T. R. *J. Am. Chem. Soc.* **1978**, *100*, 5472–5487. (c) Rogic, M. M.; Demmin, T. R.; Hammond, W. B. *J. Am. Chem. Soc.* **1976**, *98*, 7441–7443. (d) Tsuji, J.; Takayanagi, H. *J. Am. Chem. Soc.* **1974**, *96*, 7349–7350.
(3) (a) Kida, S.; Okawa, H.; Nishida, Y. In "Copper Coordination Chemistry: Biochemical and Inorganic Perspectives"; Karlin, K. D., Zubieta, J., Eds.; Adenine Press: New York, 1983; pp 425–444. (b) Bulkowski, J. E.; Summers, W. E. Reference 3a, pp 445–456. (c) Oishi, N.; Nishida, Y.; Ida, K.; Kida, S. *Bull. Chem. Soc. Jpn.* **1980**, *53*, 2847–2850. (d) Speier, G.; Tyeklar, Z. *J. Molec. Catal.* **1980**, *9*, 233–235.
(4) Thompson, J. S.; Calabrese. J. C. *Inorg. Chem.* **1985**, *24*, 3167–3171.

0002-7863/86/1508-1903$01.50/0